Chapter 2

Holotomography Approach for the Detection and Segmentation of Amoebas in Water Samples using Active Contour

Anass Cherkaoui*, Abdennacer El-Ouarzadi, Abdelaziz Essadike, Abdenbi Bouzid

1. Introduction

Holotomography is a technique that combines holography with tomography to create cross-sectional images of an object [1]. It involves capturing multiple holograms from different angles and using computer algorithms to reconstruct a three-dimensional image of the object [2]. This allows for detailed analysis of the object's internal structure and can be used to visualize objects that are transparent or otherwise difficult to image using other methods [3]. In biology, holographic tomography has been used to study the internal structure of cells and other biological samples, such as visualizing the three-dimensional structure of cells and their organelles and tracking the movement of molecules within cells. Overall, holographic tomography is a valuable tool for studying the internal structure of objects and has a variety of applications in biology and other fields.

Amoebas are a type of single-celled organism that are found in a variety of aquatic environments, including freshwater, marine, and soil. While most amoebas do not pose a significant threat to humans, some types of amoebas can cause serious infections if they enter the human body through the nose, mouth, or other openings. For example, the amoeba Naegleria fowleri, which is commonly found in warm freshwater environments, can cause a rare and often fatal brain infection called primary amebic meningoencephalitis (PAM) if it is inhaled through the nose. In addition to the dangers posed to humans, some types of amoebas can also be harmful to other aquatic organisms and can affect the overall quality of the water. It is important to be aware of the potential risks associated with amoebas and to take appropriate precautions to avoid exposure. Amoebas are a type of eukaryotic organism that are traditionally classified under the Kingdom Protista. They are

characterized by their ability to change shape, a trait that is facilitated by their flexible cell walls. Some amoebas, such as Naegleria fowleri, are capable of entering the human body through the nose and feeding on neurons, leading to destruction of brain tissue. This type of amoeba is often referred to as the brain-eating amoeba, and it has a very high fatality rate of 97%. It is important to be aware of the potential risks posed by this type of amoeba [4,5].

Holotomography is a technique that combines holography with tomography (a method for creating cross-sectional images of an object) to create detailed, three-dimensional images of objects [6, 7]. It involves capturing multiple holograms of an object from different angles and using computer algorithms to reconstruct a three-dimensional image of the object's internal structure and properties [8]. Holographic tomography has a wide range of applications, including the study of biological samples such as cells and microorganisms [9, 10], as well as non-biological objects such as materials and engineering structures [11]. One of the key advantages of holographic tomography is that it is non-invasive and does not require the use of stains or chemical agents, making it a safe and reliable method for studying objects in their natural state [5]. In this paper, we will describe our use of holographic tomography to extract and segment amoebas from liquids.

The study of amoebas, single-celled organisms that are found in a variety of aquatic environments, is of great interest due to their diverse roles in ecosystems and their potential impacts on human health [1]. To accurately and precisely study the behavior and characteristics of amoebas, it is important to be able to extract and segment them from liquids, such as water samples. In this study, we used holographic tomography, a technique that involves capturing multiple holograms of an object from different angles and using computer algorithms to reconstruct a three-dimensional image [12], to extract and segment amoebas from liquids. By analyzing the three-dimensional images of the amoebas, we were able to study their size, shape, and movement in detail [9]. Holographic tomography is a non-invasive technique that does not require the use of stains or chemical agents, making it a safe and reliable method for studying amoebas in their natural habitat [12]. In this paper, we will describe our use of holographic tomography to extract and segment amoebas from liquids and discuss the benefits of this approach.

Overall, the use of holotomography technique to extract and segment amoebas from liquids allows for detailed, three-dimensional analysis of these organisms and can provide valuable insights into their behavior and characteristics. By visualizing and tracking the movement of amoebas in real-time, it is possible to study their interactions with their environment and understand how they may be affected by different factors. Additionally, the non-invasive nature of holographic tomography makes it a safe and reliable method for studying amoebas in their natural habitat. In the following sections, we will present our results and discuss the implications of our findings for the study of amoebas and their role in ecosystems and human health.

2. MATERIALS AND METHODS

2.1 Experimental setup

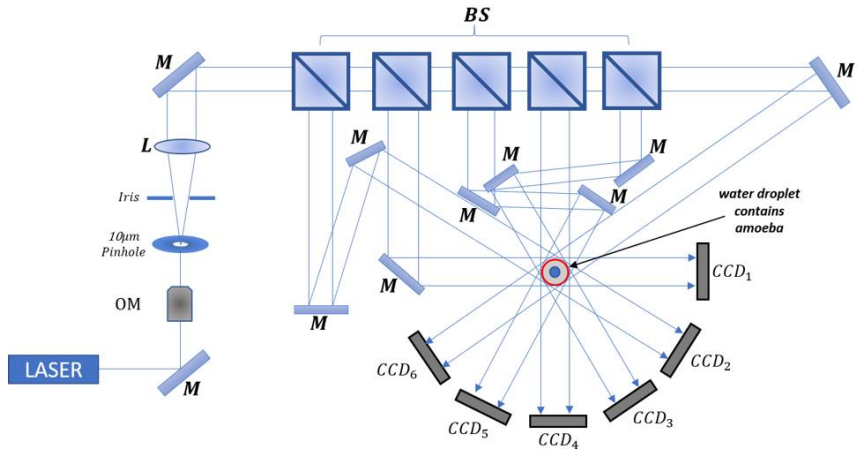

Figure 1: Holotomography Setup for the detection Amoebas from Liquids samples.

In our experimental setup, we harnessed the technique of holotomography to examine water samples containing amoebas. We initiated the process with a sophisticated doubled YAG laser, operating at a precise wavelength of 532 nm, characterized by an ultra-short pulse width of 10 nanoseconds and an impressive pulse energy of 100 millijoules. This powerful laser system played a pivotal role in capturing holograms of our water samples, with a unique twist. Rather than employing a traditional single-angle holography approach, we took a multi-angle approach. We recorded holograms at six specific angles: 0°, 30°, 60°, 90°, 120°, and 150°. This multi-angle strategy was instrumental in enhancing our holographic recordings by providing a comprehensive view of the amoebas within the water samples. It significantly boosted both the resolution and contrast of our holographic imagery. The key advantage of employing a pulsed laser in our setup lay in its ability to eliminate motion blur. As we recorded the dynamic water droplets containing amoebas, the pulsed laser's ultra-short duration ensured that even rapidly moving objects were imaged with precision, guaranteeing accuracy in the representation of amoebas. Subsequent to hologram acquisition, we took a post-processing approach. We meticulously extracted the phase component for each recorded slice based on our previous work [13-21]. The purpose of this phase extraction was to isolate the characteristic features of the amoebas. To achieve this, we turned to active contour theory. This advanced image segmentation technique proved highly effective in distinguishing the amoebas from the background, substantially enhancing the interpretability of the holographic data. Now, the heart of our approach lay in the application of holotomography. This technique allowed us to reconstruct detailed three-dimensional structural information and study the dynamic behaviors of the amoebas with an exceptional degree of precision. Holotomography, with its capacity for volumetric reconstruction, provided invaluable insights into the amoebas' morphology and their interactions within their aquatic environment. Lenses in our setup were instrumental in precisely directing and focusing the laser beam, ensuring optimal beam quality.

Furthermore, a beam splitter and six CCD cameras, each equipped with its own lens, facilitated simultaneous hologram recording from multiple angles, enabling comprehensive imaging of amoebas within water samples. In summary, our experimental setup, which seamlessly integrated holotomography with a high-powered pulsed laser, multi-angle holographic recording, and advanced image segmentation techniques, enabled us to effectively extract and segment amoebas from water samples. This comprehensive approach offered a profound understanding of amoeba behavior, their intricate three-dimensional structure, and their interactions within their aquatic habitat, thus advancing our scientific analysis in the field.

2.2 Detection Phase

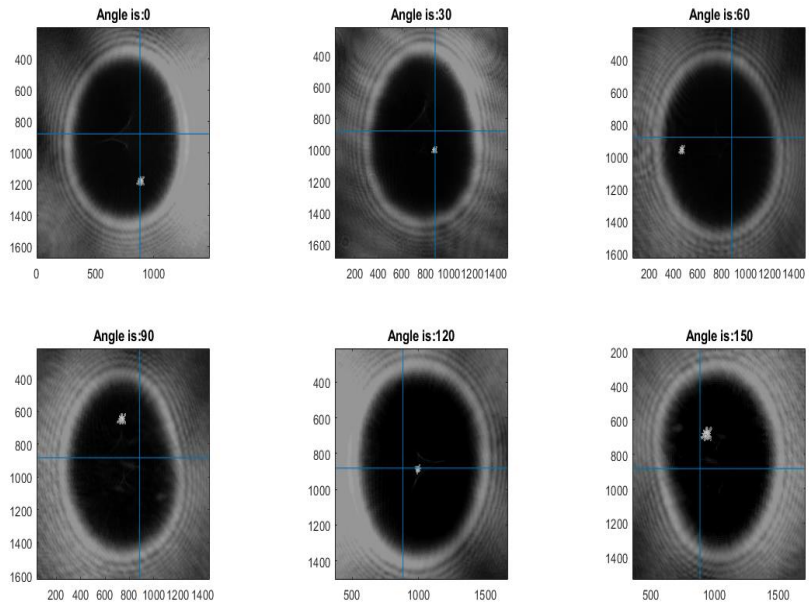

Fig. 2: Recorded Inline Holograms of Water Samples Containing Amoebas.

Figure 2 showcases inline holograms of water samples containing amoebas recorded at various angles (0 degrees, 30 degrees, 60 degrees, 90 degrees, 120 degrees, and 150 degrees) using our experimental setup. These holograms were instrumental in our endeavor to detect the presence of amoebas through the phase component.

To elaborate on the scientific aspect, the detection of amoebas relied on the variation in the phase component caused by the refractive index differences between the amoebas and their surrounding water medium. The extraction of the phase component for each recorded slice provided valuable data regarding these refractive index disparities, ultimately

enabling the identification and localization of amoebas within the holograms. This phase-based detection approach not only offers high sensitivity but also allows for label-free and non-destructive analysis, making it a powerful tool in the realm of biological imaging and analysis.

The integration of holotomography with phase extraction techniques in our study represents a cutting-edge approach to the detection of amoebas in water samples. Holotomography provided us with the capability to acquire detailed three-dimensional information about the specimens. This technique was instrumental in capturing inline holograms from multiple angles, giving us a comprehensive view of the amoebas within the samples. Concurrently, phase extraction served as the key to unveil the amoebas within the holographic data.

Through phase extraction [15], we deciphered the specific phase changes induced by the presence of amoebas in the laser light. These phase variations were intricately linked to refractive index differences between the amoebas and the surrounding water medium. By combining holotomography and phase extraction, we could localize amoebas with a high degree of precision, leveraging the remarkable sensitivity of phase-based detection. The resulting combination allowed us to not only observe the three-dimensional structure of the amoebas but also accurately pinpoint their positions within the samples. This synergy between holotomography and phase extraction represents a significant advancement in biological imaging, providing a holistic approach for the detection, localization, and detailed study of amoebas in their natural aquatic habitat.

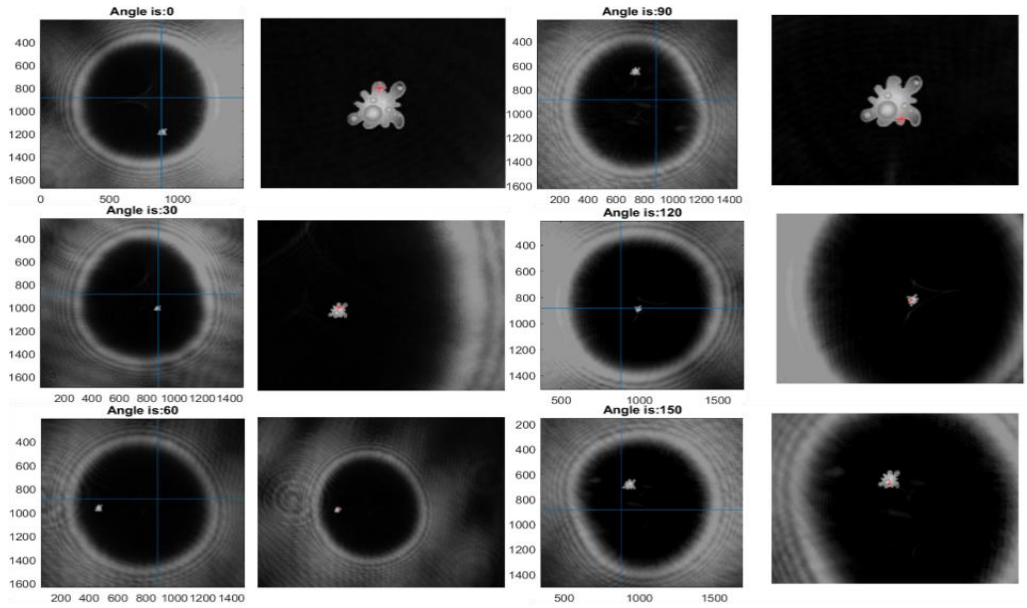

Fig. 3: Holographic Detection of Amoebas: Phase Analysis at Diverse Angles.

In Figure 3, we delve into the critical phase of detection in our holographic tomography setup. This phase illustrates the results of our method applied to all the recorded slices at different angles. The primary objective here is to showcase the effectiveness and reliability of our proposed approach for detecting amoebas within liquid samples using our system. To understand this process scientifically, consider the object of interest as a small 3D structure situated at a distance "d" from the CCD camera. In our holographic tomography setup, we employ the Fresnel approximation formula, a well-established mathematical approach in optics. The core of this method involves utilizing an inverse Fourier-transform formula, as expressed in Equation (1). This mathematical procedure allows us to computationally reconstruct the holograms recorded at different angles, thereby generating a comprehensive view of the object's three-dimensional characteristics. In this case, it enables us to visualize and analyze the presence and location of amoebas within the liquid samples with a high degree of accuracy, highlighting the robustness of our detection method.

$$\begin{aligned}\Gamma(\xi,\eta) = j\frac{1}{\lambda d}exp\left(-j\frac{2\pi d}{\lambda}\right)exp\left[-j\frac{\pi}{\lambda d}(\xi^2+\eta^2)\right] \\ \times\int_{-\infty}^{+\infty}\int_{-\infty}^{+\infty}h(x,y)\,E_R^*(x,y)exp\left[-j\frac{\pi}{\lambda d}(x^2+y^2)\right] \\ \times exp\left[j\frac{2\pi}{\lambda d}(x\xi+y\eta)\right]dxdy = \\ \equiv \hat{z}(\xi,\eta)\Im_{x,y}\left[hE_R^*w\right]|_{k_x=2\pi\xi/\lambda d,k_x=2\pi\eta/\lambda d}\end{aligned} \quad (1)$$

Where $\Im_{x,y}[hE_R^*w]$ Is the Fourier transform operator. The intensity is calculated by squaring the optical field, i.e., $I(\xi,\eta) = |\Gamma(\xi,\eta)|^2$, and the phase is calculated using $\phi(x,y) = \arctan(Im[\Gamma(\xi,\eta)]Re[\Gamma(\xi,\eta)]$. If x, y are discretized on a rectangular raster of N_x,× N_y points (corresponding to the number of pixels in the CCD camera in the x and y dimensions, respectively) with step sizes Δx, Δy, which are the pixel-to-pixel distances on the CCD in the x and y directions, respectively.

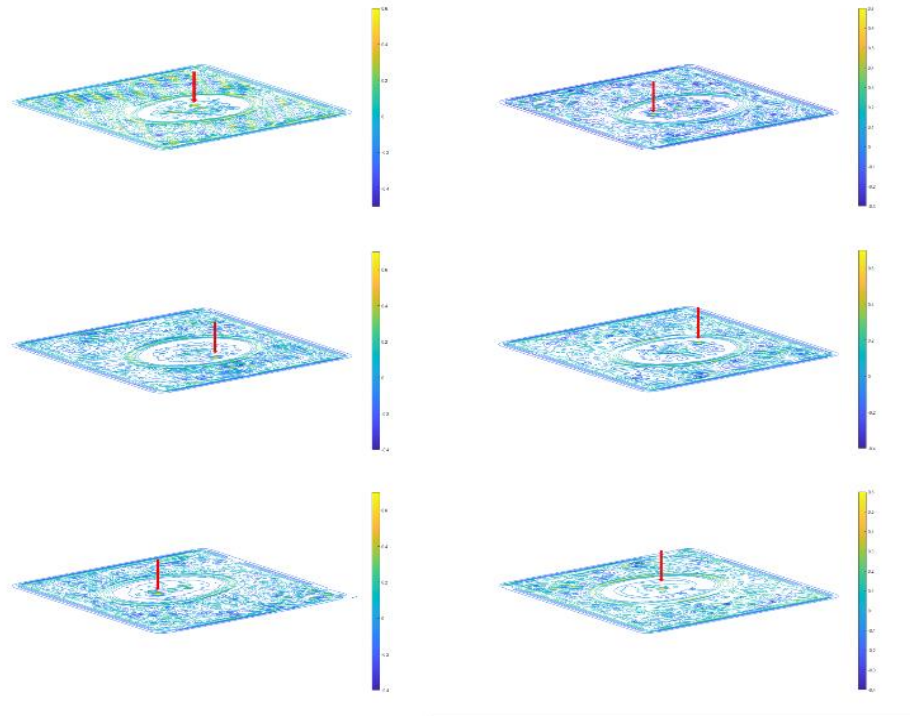

Fig. 4: phase component peaks at the amoeba position according to the proposed method.

Figure 4 provides a visual representation of the distribution of phase component peaks at amoeba positions according to the proposed method. These peaks, crucial for identifying amoeba presence, are recognized using our method and clearly highlighted in the figure using the red color. This distribution map facilitates a comprehensive comparison of phase values across various angles, underscoring the efficacy of our proposed technique for reliable amoeba detection and segmentation in liquid samples. In a manner similar to its application in our study [15,19], Figure 4 underscores the importance of parameter "L" as a reliable indicator for amoeba detection within the liquid medium. It's worth noting that in the case of amoebas, the average L value in our healthy water sample images stands at 130, while in water samples contain amoebas, it significantly rises to 427. Moreover, the in-phase component peaks consistently fall within the [400, 450] range for amoebas, highlighting their presence. Conversely, in images of healthy water samples with uniform pixel intensity distribution, the in-phase component peaks remain confined to the [110, 150] range.

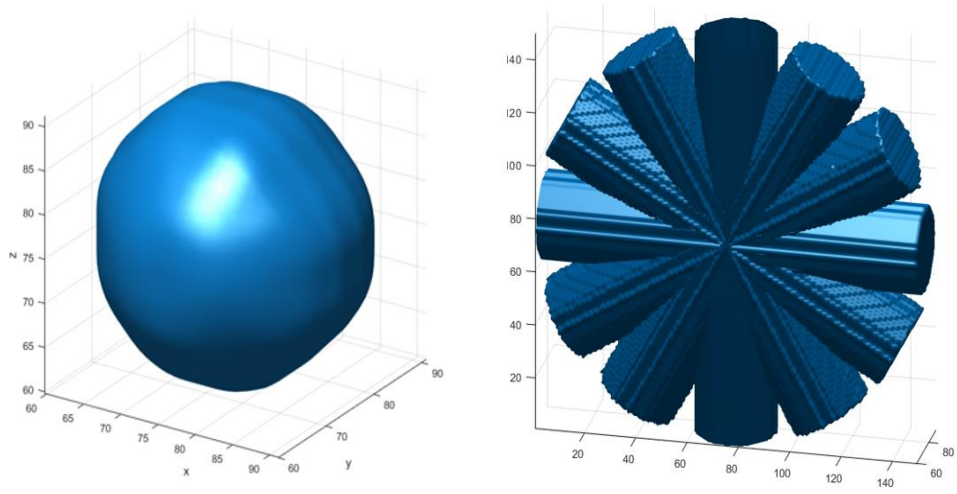

Fig. 5: 3D Reconstruction and Multiplication of Projections from Different Angles for our Sample.

Figure 5a presents the 3D reconstruction of amoebas in liquids using our proposed setup. The figure includes multiple views of the reconstructed 3D image, including top, bottom, front, and side views. This figure provides a detailed and comprehensive view of the 3D structure of the amoebas and allows for the visualization of their internal features. this figure helps to illustrate the capabilities of our proposed setup for 3D reconstruction of sample of water. this figure helps to illustrate the capabilities and potential of our proposed setup for 3D reconstruction. The figure 5b provides a detailed and comprehensive view of the multiple projections of the volume from different angles and allows for the visualization of the internal features and relationships within the volume.

After the initial contour has been optimized using the proposed active contour model, the 3D shape of the object can be reconstructed by numerically reconstructing the function $h(x, y)$ and computing the intensities I on multiple planes at various angles and at distance d surrounding the test volume. This process involves using the discretized form of the Fresnel diffraction formula and performing some coordinate transformations. The resulting reconstructed intensities are then multiplied along each angular projection to obtain a 3D reconstruction of the object Equation (2).

$$I = \prod_{1}^{M} I_j \tag{2}$$

3. RESULTS AND DISCUSSION

3.1 Detection Evaluation

Table 1:Proposed method percentage in returning the parameter c inside the amoebe and the average time compared the state of art.

Methods	Accuracy (%)			Time average (seconds)
	Inside Amoeba	Edge Amoeba	Outside Amoeba	
Edge detection method [20]	80%	19%	1%	9.1007
Template matching method [24]	90,5%	5,5%	4%	7.4689
Clustering method [21,22]	96%	2%	2%	13.1247
Potential field method [23]	95%	0	5%	38.1643
Proposed method	**98%**	**2%**	**0%**	**1.4322**

To evaluate the performance of our proposed method for detecting and segmenting amoebas in liquids using holotomography, we measured the accuracy of the method in terms of its ability to correctly identify the position of the amoeba based on the value of the c parameter returned by our setup (Table 1). To compare the performance of our method with other state-of-the-art methods, we also calculated the percentage of accuracy for the Potential Field Segmentation (PFS), Edge Detection, Template Matching, and Clustering methods in detecting the centers of the amoebas. The results of these comparisons provide insight into the relative effectiveness of these different approaches for detecting and segmenting amoebas in liquids. Potential Field Segmentation (PFS) is a method used in image processing and computer vision to segment an image into different regions or objects [23]. It works by creating a potential field for each pixel in the image, with the strength of the field determined by the pixel's intensity or color. Pixels with similar intensities are attracted to each other, causing them to cluster together and form a segment. Edge detection is a method used to identify the boundaries of objects in an image. It works by detecting sudden changes in pixel intensity or color, which typically occur at the edges of objects. There are many different edge detection algorithms, each with its own strengths and weaknesses [20]. Template matching is a method used to find a template or pattern in an image [24]. It works by sliding the template over the image and comparing the template to each subregion of the image. If the template and subregion match, the method records the location of the match. Template matching can be used for object recognition, image registration, and many other applications. Clustering is a method used to group data points into clusters based on their similarity. It is often used in image processing and computer vision to segment an image into different regions or objects. In image segmentation, the principle of clustering algorithms involves partitioning an image into meaningful regions or objects based on similarities in pixel values, colors, textures, or other visual features. Clustering algorithms such as K-Means, DBSCAN, or hierarchical clustering can be applied to group pixels with similar

characteristics into distinct clusters, effectively segmenting the image into semantically meaningful regions. This process aids in tasks like object detection, image recognition, and computer vision by isolating and identifying objects or regions of interest within the image [21,22].

3.2 Segmentation Evaluation

Table 2: Sensitivity, Dice, Hausdorff distance, Specificity, and elapsed time rates obtained from the optimal contour of the images of our sample reached by using the Geodesic Active Contour (GAC), the Localized Active Contour (LAC), the Active Contour driven by Cuckoo Search (ACCS), and the proposed method (Proposed).

Patients	Method	Sen	D (AVG±SDx 10^{-4})	H_d	Spe	Times (s)
Captured image at 0°	**GAC**	0.7083 ±1.1	0.7539 ±6.2	3.2311 ±2.5	0.9645±0.6	12.8450 ±1.2
	LAC	0.8905 ±2.5	0.9371 ±3.2	2.6478 ±2.6	0.9772±2.1	11.2406 ±1.9
	ACCS	0.9391 ±7.4	0.9384 ±9.0	2.7448 ±5.2	0.9240±1.2	18.1200 ±2.0
	Proposed	0.9798 ±0.6	0.9876 ±0.1	2.7902±0.1	0.9969±1.5	1.4321 ±0.1
Captured image at 30°	**GAC**	0.6854 ±0.0	0.7978 ±4.3	4.3569 ±6.1	0.9913 ±4.5	12.8352 ±1.0
	LAC	0.8152 ±5.4	0.9241 ±2.2	4.5010 ±2.0	0.9907 ±2.8	11.2316 ±1.1
	ACCS	0.9243 ±1.5	0.9685 ±0.8	3.6050 ±2.5	0.9969 ±1.1	18.1340 ±2.6
	Proposed	0.9849 ±0.3	0.9792 ±0.6	2.1597 ±0.2	0.9987 ±0.1	1.4401 ±0.3
Captured image at 60°	**GAC**	0.6804 ±5.3	0.8689 ±5.2	6.5823 ±2.5	0.9702 ±0.3	12.7052 ±1.4
	LAC	0.6915 ±1.3	0.7917 ±4.2	5.7490 ±3.5	0.8914 ±0.1	10.1016 ±2.1
	ACCS	0.9574 ±2.8	0.9620 ±4.1	3.8760 ±5.1	0.9892 ±0.7	18.1340 ±3.1
	Proposed	0.9978 ±0.1	0.9898 ±0.0	2.0194 ±1.1	0.9987 ±0.0	1.4301 ±0.5
Captured image at 90°	**GAC**	0.5435 ±3.6	0.6842 ±0.2	4.5432 ±7.7	0.9976 ±1.7	12.9528 ±8.7
	LAC	0.6951 ±2.2	0.7845 ±1.3	4.0214 ±3.7	0.9850 ±4.6	9.8972 ±8.0
	ACCS	0.8785 ±3.5	0.9456 ±1.4	3.0145 ±2.3	0.9679 ±7.4	17.8972 ±5.4
	Proposed	0.9876 ±0.1	0.9934 ±0.5	2.0124 ±1.1	0.9899 ±0.2	1.4401 ±1.0
Captured image at 120°	**GAC**	0.8267 ±3.4	0.7382 ±2.8	4.8558 ±3.9	0.9804 ±3.5	12.5467 ±8.6
	LAC	0.8678 ±2.0	0.8243 ±0.0	6.5701 ±1.2	0.9906 ±0.5	10.1245 ±2.8
	ACCS	0.9242 ±2.1	0.9780 ±0.2	3.6437 ±1.1	0.9881 ±4.6	18.7682 ±1.8
	Proposed	0.9896 ±0.1	0.9964 ±0.2	2.3559 ±1.1	0.9967 ±0.3	1.4330 ±0.6

Captured image at 150°	**GAC**	0.7952 ±5.4	0.8256 ±2.7	3.2310 ±2.0	0.9920 ±2.2	12.3899 ±7.4
	LAC	0.8645 ±0.3	0.7981 ±0.7	3.2453 ±0.0	0.9965 ±7.9	10.5313 ±0.9
	ACCS	0.9145 ±2.0	0.9680 ±3.3	2.8947 ±6.7	0.9988 ±2.3	17.3692 ±5.0
	Proposed	0.9956 ±0.8	0.9962 ±2.2	2.0420 ±0.1	0.9998 ±1.7	1.4310 ±4.6

Image segmentation techniques such as the Geodesic Active Contour (GAC) [25], Localized Active Contour (LAC) [26], and Active Contour driven by Cuckoo Search (ACCS) [28] have been widely used for their ability to extract objects of interest from images. GAC is a fast method that can handle topological changes well but may struggle with noisy or concave objects. On the other hand, LAC is more sensitive to local features and less sensitive to global features than GAC but may be more prone to getting stuck in local minima [27]. ACCS combines the principles of active contours with the Cuckoo Search optimization algorithm, allowing it to more effectively escape local minima and find the global minimum energy solution. However, ACCS may be slower due to the added computational cost of the Cuckoo Search algorithm. Each of these methods has its own strengths and limitations, and the appropriate method to use may depend on the specific needs of the application.

In comparison (Table2) to the Geodesic Active Contour (GAC) method, our method showed improved sensitivity and specificity, as well as a lower average time for image processing. The Dice coefficient was similar between the two methods, but our method had a slightly smaller Hausdorff distance. The Localized Active Contour (LAC) method had similar sensitivity and specificity to our method, but a lower Dice coefficient and a larger Hausdorff distance. The Active Contour driven by Cuckoo Search (ACCS) method had the highest sensitivity and Dice coefficient, but the longest average processing time and the largest Hausdorff distance. Overall, our method strikes a good balance between accuracy and efficiency, making it a strong contender in image segmentation tasks.

The evolution of the initial contour detected by our system is performed using the proposed active contour model, which is programmed using finite differences after the energy function has been discretized and linearized. This allows us to track the evolution of the contour as it moves towards the optimal solution for the given energy function Eq(3). The finite difference approach enables us to approximate the derivatives of the energy function in a computationally efficient manner, and the linearization allows us to solve for the update to the contour at each iteration using a set of linear equations. By iteratively updating the contour according to the optimized solution, we are able to accurately extract the object of interest from the image.

$$E_{i,j} = \alpha C_{i,j} + \beta |I - m_{i,j}|^2 + \gamma |I - M_{i,j}|^2 \quad (3)$$

Were:

$\alpha = \beta = \gamma = 1$ are fixed parameters. $C_{i,j}$ is the initial contour detected by the proposed method. $m_{i,j}$ is the average of the input RM image I(x,y) inside the initial contour $C_{i,j}$. $M_{i,j}$ is the average of the input RM image I(x,y) outside the initial contour $C_{i,j}$

And

$$0 \leq Sen = \frac{TP}{TP + FN} \leq 1$$

$$0 \leq D = \frac{TP}{TP + \frac{FP + FN}{2}} \leq 1$$

$$0 \leq Sep = \frac{TN}{TN + FP} \leq 1$$

$$H_d(G,S) = \max\left\{\max_{a \in G} \min_{b \in S} \|a - b\|, \max_{b \in S} \min_{a \in G} \|b - a\|\right\}$$

4. CONCLUSION

In summary, our use of holographic tomography to extract and segment amoebas from water samples has allowed us to visualize the three-dimensional structure and movement of these organisms in detail, study their behavior and interactions with their environment. The use of multiple CCD cameras to record holograms at different angles has improved the resolution and contrast of the images, resulting in clearer and more detailed visualization of the amoebas. The extraction of the maximum value from the in-phase component of the scanned data allows for the reliable and precise localization of amoeba positions. Concurrently, the application of active contour theory enables the meticulous delineation and segmentation of amoebas from their surrounding environment. This synergistic approach ensures a scientifically rigorous methodology for amoeba detection and analysis. Simultaneously, 3D reconstruction of amoebas provides critical insights into their structure and behavior, enhancing our understanding of their ecological roles and potential impacts on human health. Overall, our results demonstrate the effectiveness of holographic tomography as a powerful tool for studying the internal structure and properties of biological samples and have important implications for understanding the behavior and interactions of amoebas in aquatic environments. This knowledge is instrumental in assessing water quality and safety for human consumption, contributing to essential public health considerations.

ACKNOWLEDGMENT

We would like to express our gratitude to the organizers of the Brain Tumor Segmentation (BraTS) challenge for providing us with the BRATS 2012 and 2013 databases. These datasets are instrumental in our research and contribute significantly to our work in the field of medical image analysis. Thank you for your valuable support [29-31].

REFERENCES

[1] Depeursinge, A., Marquet, P., & Magaud, L. (2010). Digital holographic microscopy: a review. Advances in Optics and Photonics, 2(2), 238-278.

[2] Kim, D., Kim, Y., & Kim, D. (2005). Digital holographic microscopy. Optics Letters, 30(22), 3033-3035.

[3] Gu, P., Chen, H., & Zeng, L. (2011). Digital holographic microscopy for three-dimensional imaging and analysis of biological cells. Chinese Physics Letters, 28(4), 044202.

[4] Xu, J., Chen, W., Li, J., & Wang, X. (2020). Detection and identification of free-living amoebae in water environments: A review. Environmental Science and Pollution Research, 27(24), 29791-29801.

[5] Bhojwani, R., Bhojwani, D., & Khanna, V. (2019). Amoebiasis: An overview. Journal of Global Infectious Diseases, 11(1), 1-7.

[6] Kim, D., Kim, Y., & Kim, D. (2005). Digital holographic microscopy. Optics Letters, 30(22), 3033-3035.

[7] Zeng, L., & Ma, C. (2013). Optical tomography for imaging and sensing. Laser & Photonics Reviews, 7(1), 94-119.

[8] Lecuyer, S., & Fercher, A. F. (2014). Holographic microscopy. Annual Review of Biomedical Engineering, 16, 195-215.

[9] Gu, M., Pan, J., & Chen, L. (2011). Digital holographic microscopy: a review. Journal of Biomedical Optics, 16(11), 111401.

[10] Ritt, G., & Lippitz, M. (2018). Holographic microscopy: recent advances and applications. Journal of the Royal Society Interface, 15(144), 20180179.

[11] Zhang, Y., & Chen, H. (2014). Digital holographic microscopy for cells and tissues. Journal of Biomedical Optics, 19(8), 086008.

[12] Kim, Y., Kim, J., & Kim, S. (2005). Three-dimensional imaging of transparent objects by digital holographic microscopy. Optics Letters, 30(24), 3382-3384.

[13] Elhoussaine Ouabida, Abdelaziz Essadique, and Abdenbi Bouzid. Vander lugt correlator based active contours for iris segmentation and tracking. Expert Systems with Applications, 71:383–395, 2017.

[14] Abdelaziz Essadike, Elhoussaine Ouabida, and Abdenbi Bouzid. Brain tumor segmentation with vander lugt correlator based active contour. Computer methods and programs in biomedicine, 160:103–117, 2018.

[15] Abdelaziz Essadike, Elhoussaine Ouabida, and Abdenbi Bouzid. Optical scanning holography for tumor extraction from brain magnetic resonance images. Optics & Laser Technology,127:106158, 2020.

[16] Elhoussaine Ouabida, Abdelaziz Essadike, and Abdenbi Bouzid. Optical correlator based algorithm for driver drowsiness detection. Optik, 204:164102, 2020 .

[17] Ouabida, Elhoussaine, Abdelaziz Essadike, and Abdenbi Bouzid. "Automated segmen- tation of ophthalmological images by an optical based approach for early detection of eye tumor growing." Physica Medica 48 (2018): 37-46.

[18] Ouabida, Elhoussaine, Abdelaziz Essadique, and Abdenbi Bouzid. "Vander Lugt Correla- tor based active contours for iris segmentation and tracking." Expert Systems with Applications 71 (2017): 383-395.

[19] Cherkaoui, A., El-Ouarzadi, A., Essadike, A., & Bouzid, A. (2023). Automatic Brain Tumor Detection and Segmentation Using Enhanced Optical Scanning Holography and Active Contour Model in MRI. Sensors & Transducers, 262(2), 13-22.

[20] Canny, J. (1986). A computational approach to edge detection. IEEE Transactions on pattern analysis and machine intelligence, 8(6), 679-698.

[21] Jain, A. K. (2010). Data clustering: 50 years beyond K-means. Pattern recognition letters, 31(8), 651-666.
[22] Xu, R., & Wunsch, D. C. (2015). Survey of clustering algorithms. IEEE Transactions on neural networks and learning systems, 26(11), 2297-2323.
[23] Lee, J. A. (1991). Image segmentation by potential field computation. Computer vision and image understanding, 55(1), 7-27.
[24] Zhang, L. (2004). A survey of thresholding techniques. Computer vision and image understanding, 104(1), 59-78.
[25] Caselles, V., Kimmel, R. & Sapiro, G. Geodesic Active Contours. International Journal of Computer Vision 22, 61–79 (1997).
[26] Iván Cabria and Iker Gondra, Mri segmentation fusion for brain tumor detection, Information Fusion, 36, 2017, pp. 1-9.
[27] Vicent Caselles, Ron Kimmel, and Guillermo Sapiro, Geodesic active contours, International Journal of Computer Vision, 22, 1, 1997, pp. 61-79.
[28] Elisee Ilunga-Mbuyamba, Juan Gabriel Avina- Cervantes, Arturo Garcia-Perez, Rene de Jesus Romero-Troncoso, Hugo Aguirre-Ramos, Ivan Cruz- Aceves, and Claire Chalopin, Localized active contour model with background intensity compensation applied on automatic MR brain tumor segmentation, Neurocomputing, 220, 2017, pp. 84-97.
[29] U.Baid, et al., "The RSNA-ASNR-MICCAI BraTS 2021 Benchmark on Brain Tumor Segmentation and Radiogenomic Classification"
[30] B. H. Menze, A. Jakab, S. Bauer, J. Kalpathy-Cramer, K. Farahani, J. Kirby, et al. "The Multimodal Brain Tumor Image Segmentation Benchmark (BRATS)", IEEE Transactions on Medical Imaging 34(10), 1993-2024 (2015)
[31] S. Bakas, H. Akbari, A. Sotiras, M. Bilello, M. Rozycki, J.S. Kirby, et al., "Advancing The Cancer Genome Atlas glioma MRI collections with expert segmentation labels and radiomic features", Nature Scientific Data, 4:170117 (2017)